LIGO-T960084-00-D

MASSACHUSETTS INSTITUTE OF TECHNOLOGY
Gravitation and Cosmology Research Group
Cambridge, Massachusetts 02139

MIT GRAVITY GRP. FAX #617-253-7014
CONFIRMATION # 617-253-4824

Facsimile Cover Sheet

DATE: 4/4/96 TIME: ________ (E.T.)

TO: BETTY BEHNKE FOR VIBRATION ISOLATION PEOPLE FROM HYTEC

FAX#: ________

ADDRESS: ________

NUMBER OF PAGES (including this cover sheet): ____

FROM: R. WEISS OFFICE #: (617)253-________

Massachusetts Institute of Technology
Room 20B-145
Cambridge, Massachusetts 02139

NOTES:

1) CONSTRAINED LAYER PAPER PLUNKETT + LEE

2) CONSTRAINED DAMPING FROM SHOCK + VIBRATION HANDBOOK CAREE

3) E GLASS FIBER IN S.S. TUBE
A + M COMPOSITES MARLBORO, MASS

4) CONTACT AT MCI - HEX CELL

12.7, 12.3i

Received 10 March 1969

Length Optimization for Constrained Viscoelastic Layer Damping

R. PLUNKETT AND C. T. LEE

Department of Aeronautics and Engineering Mechanics, University of Minnesota, Minneapolis, Minnesota 55455

Viscoelastic materials are used extensively to damp flexural vibrations of metallic structures; it has been known for some time that the energy dissipation due to shear strain in the viscoelastic layer can be increased by constraining it with a stiffer covering layer. In this paper, we will discuss a method for increasing this damping by cutting the constraining layer into appropriate lengths. The analysis for a single layer of this treatment is relatively straightforward. The damping can be increased still further by using several layers; in this case, the analysis is based upon effective complex elastic moduli of an equivalent homogeneous medium. One result found from this analysis is that, if the element length of the constraining layer is optimum, the damping depends primarily upon the stiffness of the constraining layer and the loss coefficient of the viscoelastic material, and only indirectly on the shear modulus of the viscoelastic layer. Experimental data is presented for comparison with the theoretical predictions.

LIST OF SYMBOLS

- D characteristic length in single layer $=(t_1t_2E_2/G_1^*)^{\frac{1}{2}}$ (in.)
- C^{*2} $=G_E^*/E_E^*$
- d thickness of the beam (in.)
- E_2 modulus of elasticity of the constraining material (psi)
- E_b modulus of elasticity of the basic structure (psi)
- E_E^* effective elastic modulus of the equivalent homogeneous material (psi)
- f natural frequency $=\omega/2\pi$ (cycles/sec)
- G_1^* complex shear modulus of the viscoelastic material (psi)
- G_1' storage shear modulus (psi)
- G_1'' loss shear modulus (psi)
- G_E^* effective shear modulus of the equivalent homogeneous material (psi)
- H total thickness of the surface treatment $=m(t_1+t_2)$ (in.)
- i $=(-1)^{\frac{1}{2}}$
- I moment of inertia of the basic structure (in.^{4})
- l length of the beam (in.)
- L total length of the surface treatment (in.)
- L_0^* characteristic length in multiple layer treatment (in.)
- L_1 element length of the constraining layer
- m number of layers of the surface treatment (integer)
- n number of elements of the constraining layer $=L/L_1$
- t time (sec)
- t_1 thickness of the viscoelastic layer (in.)
- t_2 thickness of the constraining layer (in.)
- u_0 displacement at the interface of the basic structure and the viscoelastic layer in the x direction (in.)
- w dimensionless length ratio
- W^* strain energy of a system (in.lb)
- $(W)_B$ energy stored in the bare specimen (in.lb)
- $(W)_S$ energy stored in a system (in.lb)
- W_{nom} nominal energy stored in a material (in.lb)
- ΔW damping energy dissipation in a material (in.lb/cycle)
- (ΔW_B) energy dissipation in the bare specimen (in.lb/cycle)
- $(\Delta W)_L$ energy dissipation in the constrained viscoelastic layers (in.lb/cycle)
- $(\Delta W)_S$ energy dissipation per cycle of a system (in.lb/cycle)
- α^* $=L_1/2L_0^*$
- β^* dimensionless ratio $=(L/H)\cdot(\pi/4)C^*$
- γ shear strain in the viscoelastic layer

γ_E^*	effective shear strain of the equivalent homogeneous material
δ	logarithmic decrement
ϵ_0	uniform strain at the interface
ϵ_E^*	effective normal strain of the equivalent homogeneous material
ζ	damping ratio $=(\log_e 10/40\pi f)\cdot(d(dB)/dt)$
η_1	dimensionless loss coefficient
η_B	loss coefficient of the bare specimen $=[(\Delta W)_B/2\pi(W)_B]$
η_G	loss tangent of the viscoelastic material $=G_1''/G_1'$
η_L	modified loss coefficient of the system $=[(\Delta W)_L/2\pi(W)_S]$
η_S	loss coefficient of a system $=[(\Delta W)_S/2\pi(W)_S]$
θ	loss angle of the viscoelastic material $=\tan^{-1}\eta G$
ξ	dimensionless length ratio $=L_1/L_0$
σ	normal stress in the constraining layer (psi)
σ_E^*	effective axial stress in the equivalent homogeneous material (psi)
τ	shear stress in the viscoelastic layer (psi)
τ_E^*	effective shear stress in the equivalent homogeneous material (psi)
ω	natural frequency (rad/sec)

INTRODUCTION

This paper discusses the optimization of constrained viscoelastic-layer damping for engineering structures such as beams, columns, and plates. For such structures, the amount of damping for a given viscoelastic layer depends on the stiffness of the constraining layer. It also depends on an effective length for the constraining layer; this effective length may be related to the bending wavelength, as it was by Kerwin,[1] or it may be created by cutting the constraining layer at regular intervals as was shown by Parfitt.[2] Lazan *et al.*[3] showed that the amount of damping can be increased by using alternately anchored multiple-layer treatment; in this paper we show that, when properly assembled, the constraining layers need not be anchored. An analysis, based on technical theory, for finite length and thickness of treatment is presented, and the predictions of this theory are compared with experimental results for one to eight layers on a cantilever beam.

Viscoelastic damping layers can be used on the surface of structural members, so that under cyclic loading the viscoelastic layer experiences the cyclic extensional strains of the surface of the member.[4,5] In the case of free viscoelastic layers, the shear strain and the dilatation in the viscoelastic layer are of the same order. If the viscoelastic layer is constrained by a stiff covering layer, it experiences large shear strain and relatively small dilatation when the member to which it is attached is strained.[5,6] Since most of the energy dissipation is caused by shear deformation and almost none is caused by dilation,[6] constrained viscoelastic layers are therefore capable of higher damping than unconstrained viscoelastic layers.

Kerwin[1] analyzed the damping of a composite structure with an infinitely long damping layer subjected to sinusoidal variation in bending moment. He found that the calculated damping factor depends on the wavelength of bending waves in the damped structure as well as on the material properties and the geometry. Parfitt[2] determined the change in damping caused by cutting the damping tape at regular intervals; his analysis is valid only for materials with small loss coefficient, since he neglected the difference between the absolute value of the shear modulus of the viscoelastic material and its real part. Lazan[3] gave an analysis of an alternately anchored multiple-layer surface treatment which was developed for increasing damping.

In this paper, we consider the case of finite-length surface treatment of an engineering structure with uniform surface strain and cyclic loading conditions. The constraining layer of the surface treatment is cut into appropriate lengths. If the constraining layer is very long, the shear stress near the ends induces the same axial strain in it as in the basic structure; thus there is no shear in the viscoelastic layer away from the ends and the damping is small. If the length of each element of the constraining layer is very short, it exerts no constraint on the underlying viscoelastic layer, there is little shear strain, and the damping is small. At some finite value for the lengths of the elements of the constraining layer, the damping is a maximum.

An analysis based upon the technical theory of elasticity is developed in a straightforward manner for a viscoelastic layer constrained by a single stiff layer but at appropriate intervals. For multiple-layer surface treatment, there are interactions between the constraining layers and the viscoelastic layers on each side. The governing equations of equilibrium can still be written for each individual layer, but solving this set of equations for a large number of layers would be very tedious. In order to simplify the analysis for the multiple-layered treatment, we replace a typical repetitive volume by an equivalent homogeneous material with the same force–deformation relationship. A longitudional elastic modulus and a transverse shear modulus is found for this equivalent material in terms of the actual physical properties and geometry of the typical volume of the original composite. This equivalent analysis gives valid results if the composite has dimensions which are large in comparison with those of an element of the constraining layer and if the strain in the basic structure does not vary too rapidly with length.

I. SINGLE-LAYER THEORY

The damping of a mechanical system under steady-state or slowly decaying vibrations can be expressed

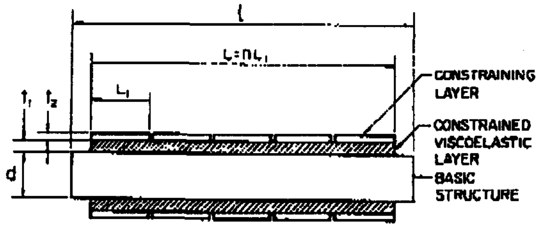

FIG. 1. Composite structure with surface treatment.

in a dimensionless form by the loss coefficient, η_S, which is the ratio of the energy dissipated per radian to the maximum strain energy in the system. That is,

$$\eta_S = \Delta W_S / 2\pi W_S,$$

where ΔW_S is the energy dissipated per cycle and W_S is the total strain energy for the entire system at maximum displacement. For linear single-degree-of-freedom systems which are lightly damped, η_S is simply related to the common measures of damping, such as logarithmic decrement δ and damping ratio ξ (Ref. 7):

$$\eta_S = 2\zeta = \delta / \pi.$$

In this study, we apply constrained damping layers to both surfaces of the basic structure. This will give us a symmetric configuration which is simpler to analyze and the general result will be the same as for a single-surface treatment. We assume that all of the damping in the constrained viscoelastic layer is attributable to shear strain and the resultant energy dissipation. The ability of the constraining layer to induce shear strain in the constrained layer without itself experiencing excessive stretching is one of the important characteristics of the damping configuration.

To study the interaction between the axial strain in the constraining layer and the shear strain in the constrained layer, we consider the case of the constraining layer cut at regular intervals (Fig. 1).

The following assumptions are made in the analysis which follows:

(1) The thickness of the constraining layer and of the constrained layer are very small compared to that of the basic structure; thus, the bending effects in these layers are negligible, so that the constraining layer is subjected to tension only and the constrained layer is subjected to shear only.

(2) We assume linear behavior of the viscoelastic material; complex notation can be used for its shear modulus $G_1^* = G_1' + iG_1'' = G_1'(1 + i\eta_G) = G_1(\cos\theta + i\sin\theta)$, where the asterisk indicates a complex quantity and where G_1' is the elastic or storage modulus, G_1'' is the loss modulus, $\theta = \tan^{-1}\eta_G$, and η_G is the loss tangent of the viscoelastic material.

(3) The constraining material is elastic and dissipates no energy. Its Young's modulus is purely real. $E_2'' = 0$ and $E_2 = E_2'$.

(4) Poisson ratio effects are negligible and the one-dimensional problem only is considered.

(5) The axial strain is uniform at the interface of the basic structure and the viscoelastic layer.

(6) Uniform shear strain is assumed through the thickness of the viscoelastic layer.

(7) Uniform normal stress is assumed through the thickness of the constraining layer.

(8) The elastic moduli of the viscoelastic layer are small in comparison with those of the constraining layer.

It is convenient to use a local coordinate system for which the origin of the abscissa is at the center of one element of the constraining layer; the origin of the ordinate is immaterial for this analysis, and it may be taken at the interface of the basic structure and the viscoelastic layer [Fig. 2(a)].

From the equilibrium of an element of the constraining layer [Fig. 2(c)], we can write the equation of equilibrium in terms of the average normal stress:

$$(\partial\sigma/\partial x)\cdot t_2 = \tau. \tag{1}$$

Since we have assumed that the problem is one-dimensional and that the shear strain in the constrained layer is uniform through the thickness of the viscoelastic layer, the stress–strain relations for the constraining layer and for the constrained layer are

$$\sigma = E_2\epsilon_x = E_2\cdot(\partial u/\partial x) \tag{2}$$

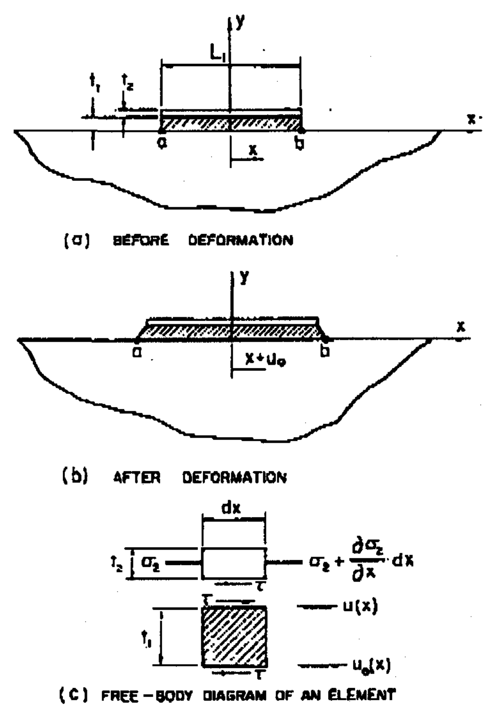

FIG. 2. Typical element of constrained viscoelastic layer applied to a basic structure.

and

$$\tau^* = G_1^*\gamma^* = G_1^*\cdot[(u^*-u_0)/t_1], \qquad (3)$$

respectively.

From Assumption 5,

$$u_0 = \epsilon_0\cdot x,$$

where ϵ_0 is the uniform strain in the basic structure, varying sinusoidally in time due to cyclic vibration of the system.

Substituting Eqs. 2 and 3 into Eq. 1, we obtain the differential equation

$$B_0^{*2}\cdot(\partial^2 u^*/\partial x^2) - u^* = -\epsilon_0\cdot x, \qquad (4)$$

where $B_0^* = (t_1 t_2 E_2/G_1^*)^{\frac{1}{2}}$ is a constant which has the dimension of length and is characteristic of the system.

The boundary conditions for one element of the constraining layer are

$$\partial u^*/\partial x = 0$$

at

$$x = \pm\frac{L_1}{2} \qquad (5)$$

since there is no normal stress at the ends.

The general solution of Eq. 4 satisfying boundary conditions (Eq. 5) is:

$$u^*(x) = \epsilon_0\left[x - B_0^*\cdot\frac{\sinh(x/B_0^*)}{\cosh(L_1/2B_0^*)}\right]. \qquad (6)$$

The energy dissipated per cycle per unit volume of a material in uniform shear is the area within the shear stress–shear strain hysteretic loop.

Since we have assumed that the shear strain is uniform through the thickness of the viscoelastic layer, the energy dissipated per cycle per unit length and width is

$$d(\Delta W) = \pi t_1 G_1''\gamma^2,$$

where γ is the absolute value of γ^* as given by Eq. 3. Using the value of u^* from Eq. 6 in Eq. 3. gives

$$d(\Delta W) = \pi t_1 G_1''\frac{\epsilon_0^2}{t_1^2}B_0^2\left|\frac{\sinh(x/B_0^*)}{\cosh(L_1/2B_0^*)}\right|^2 \qquad (7)$$

Writing G_1'' in the form $G_1''=G_1\sin\theta$ in the definition of B_0^*, using the trigonometric identities for the functions sinh and cosh of a complex argument, and integrating over the length of one element of the constraining layer yields

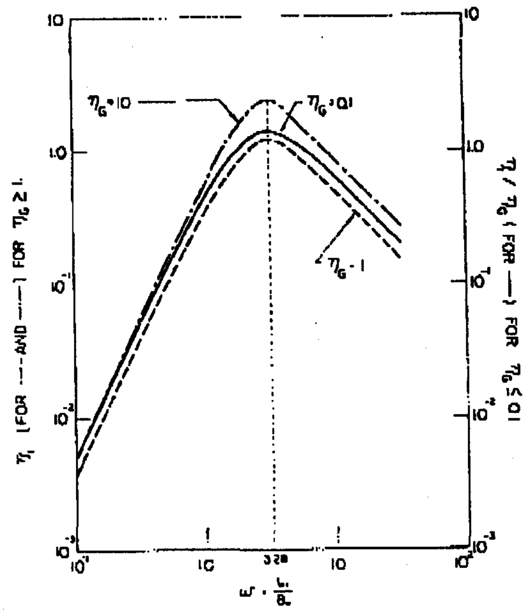

FIG. 3. η_1 versus $w=L_1/B_0$ for single constraining layer.

$$\Delta W = 2\pi\epsilon_0^2 t_2 E_2 L_1\cdot\frac{1}{\omega}\left[\frac{\sinh[\omega\cdot\cos(\theta/2)]\cdot\sin(\theta/2) - \sin[\omega\cdot\sin(\theta/2)]\cdot\cos(\theta/2)}{\cosh[\omega\cdot\cos(\theta/2)]+\cos[\omega\cdot\sin(\theta/2)]}\right], \qquad (8)$$

where $w = L_1/B_0$ is a dimensionless ratio. This can be made dimensionless by dividing by a nominal energy appropriate to the system:

$$W_{nom} = \tfrac{1}{2}\epsilon_0^2 E_2 t_2 L_1. \qquad (9)$$

This would be the maximum strain energy in an element of the constraining layer if the whole layer were strained by an amount ϵ_0. With this definition, the dimensionless loss coefficient is

$$\eta_1 = \frac{\Delta W}{W_{nom}} = 4\pi\cdot\frac{1}{\omega}\left[\frac{\sinh(A)\cdot\sin(\theta/2) - \sin(B)\cdot\cos(\theta/2)}{\cosh(A)+\cos(B)}\right], \qquad (10)$$

where $A = w\cdot\cos(\theta/2)$, $B = w\cdot\sin(\theta/2)$, and θ is the loss angle of the viscoelastic material.

Equation 10 shows that η_1 is a function of w and η_G only. η_1 is plotted as a function of w in Fig. 3, with η_G as a parameter. For $\eta_G<1$, η_1 is almost linearly proportional to η_G and, for $\eta_G>1$, η_1 is almost independent of η_G. But for all values of η_G, η_1 is a maximum at about

$$w = L_1/B_0 = 3.28;$$

thus, for a given viscoelastic layer and constraining layer, for maximum damping, the length of each element of the constraining layer, L_1, is 3.28 times the characteristic length, B_0, of the system.

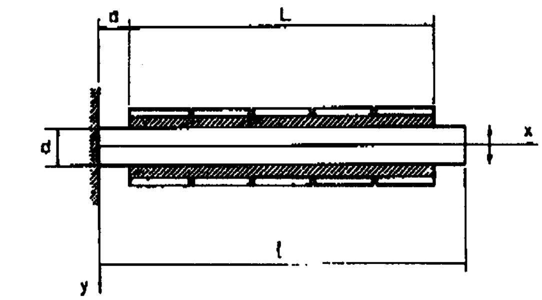

FIG. 4. Cantilever beam with surface treatment.

In order to compare with experimental results, we consider the case of a cantilever beam subjected to sinusoidal flexural vibration with small deformation, Fig. 4; the strain at the interface is

$$\epsilon_0 = -(d/2)\cdot(d^2y/dx^2), \tag{11}$$

where d is the thickness of the beam and d^2y/dx^2 is the curvature of the beam. Integrating over the length of the surface treatment yields

$$\Delta W_L = 2\int_a^{a+L} \frac{\Delta W}{L_1}\cdot dx = 2\int_a^{a+L} \eta_1 \cdot \frac{W_{\max}}{L_1}\cdot dx = \eta_1\cdot\frac{d^2}{4}E_2\cdot t_2 \int_a^{a+L}\left(\frac{d^2y}{dx^2}\right)^2\cdot dx. \tag{12}$$

The factor 2 takes care of surface treatment on both faces of the basic structure.

The maximum strain energy in the system is

$$W_S = \frac{E_b d^3}{24}\int_0^l \left(\frac{d^2y}{dx^2}\right)^2\cdot dx, \tag{13}$$

where E_b is the Young's modulus of the basic material. From Eqs. 12 and 13 we obtain the modified loss coefficient of the system:

$$\eta_L = \frac{\Delta W_L}{2\pi W_S} = \eta_1\cdot\frac{3E_2 t_2}{\pi E_b d}\int_a^{a+L}\left(\frac{d^2y}{dx^2}\right)^2\cdot dx \Big/ \int_0^l \left(\frac{d^2y}{dx^2}\right)^2\cdot dx. \tag{14}$$

In order to compare the experimental results, we can substitute the expression for the curvature of a uniform cantilever vibrating at its fundamental mode[3] into Eq. 14 and evaluate the integrals explicitly. The modified loss coefficient of the system η_L can then be found in terms of η_1 (Eq. 10), and the geometry and material properties of the beam and the constraining layer.

Equation 14 shows that the loss coefficient of the system depends on the loss coefficient of the viscoelastic material, the stiffness of the constraining layer, and the stiffness of the basic structure. It does not depend explicitly on the shear modulus of the constrained viscoelastic material. The above integral is evaluated for an explicit case in Sec. III and the results are compared with measured values.

II. MULTIPLE-LAYER THEORY

The amount of damping in structures studied in the previous section can be increased by applying more than one constrained viscoelastic layer to the surface of the basic structure, as shown in Fig. 5.

If there is more than one constrained viscoelastic layer, there are constraining layers on both sides of the viscoelastic layer and interactions are induced between them. The governing equations of equilibrium can still be written for each individual layer, but to solve this set of equations for a large number of layers would be tedious. For convenience, we replace a repetitive element which is typical of the multiple-layered treatment by an equivalent homogeneous orthotropic material with the same force-deformation relationship. The equilibrium condition for this typical volume is shown in Fig. 6.

We follow the same assumptions made for single layer analysis in Sec. I. From the equilibrium of an element of the viscoelastic layer we have the differential equation of equilibrium in the x direction:

$$\partial\sigma/\partial x + \partial\tau/\partial y = 0. \tag{15}$$

Since the strain for the constraining layer ϵ_2 is of the same order as the strain for the viscoelastic layer ϵ_1 and $E_2 \gg E_1$ (Assumption 8), then $\sigma_2 \gg \sigma_1$, and σ_1 is negligible (Assumption 1).

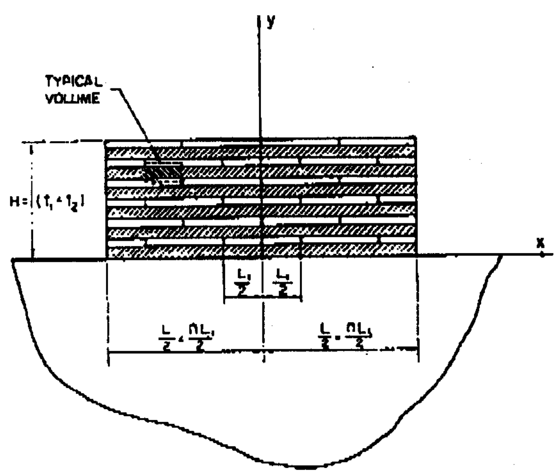

FIG. 5. Multiple-layer surface treatment.

With
Then u.
linear ir
From Fi
i.e.,
If $f_1(x)$
in x, Eq
which is
Substitu
librium
and, usi
ing laye
$t_1t_2\cdot(E_2$
The l
fore, the
is antis
therefor
and
where
which h
solutions
$u^*(x$
The con
boundar
(i) Su
(ii) Th
and Eq.
$u^*($
This is t
x directi
We n
with the
nonhom
gible; th

With these assumptions, τ is constant in y and so is γ. Then u, the deformation in the x direction, must be linear in y, and we can write $u(x,y)$ in the form

$$u(x,y) = y \cdot f_1(x) + f_2(x). \quad (16)$$

From Fig. 6(b), the axial deformation is antisymmetric; i.e.,

$$u(x,y) = -u(-x, -y).$$

If $f_1(x)$ is symmetric in x and $f_2(x)$ is antisymmetric in x, Eq. 16 is the most general antisymmetric function which is linear in y. Then

$$\gamma(x) = \partial u/\partial y = f_1(x). \quad (17)$$

Substituting Eqs. 16 and 17 into the equation of equilibrium for the constraining layer gives

$$(\partial\sigma/\partial x)\cdot(t_2/2) = \tau,$$

and, using the stress-strain relations for the constraining layer and the viscoelastic layer, we get

$$t_1 t_2 \cdot (E_2/4G_1^*) f_1''(x) - f_1(x) = -(E_2 t_2/2G_1^*) f_2''(x) \quad (18)$$

The left-hand side is symmetric by definition; therefore, the right-hand side must be symmetric. But $f_2''(x)$ is antisymmetric unless it is zero. Equation 18 is therefore:

$$\tfrac{1}{4} L_0^{*2} f_1''(x) - f_1(x) = 0$$

and

$$f_2''(x) = 0,$$

where $L_0^* = (t_1 t_2 E_2/G_1^*)^{1/2}$ is a system characteristic which has the dimension of length. The appropriate solutions give

$$u^*(x, t_1/2) = (A_1 \cdot t_1/2)\cosh(2x/L_0^*) + A_2 x. \quad (19)$$

The constants A_1 and A_2 are evaluated from the boundary conditions:

(i) Stress at $(L_1/4, t_1/2)$ is σ_0,

$$(\partial u^*/\partial x)(L_1/4, t_1/2) = \sigma_0/E_2;$$

(ii) The end $(-L_1/4, t_1/2)$ is stress free,

$$(\partial u/\partial x)(-L_1/4, t_1/2) = 0;$$

and Eq. 19 becomes

$$u^*\left(x, \frac{t_1}{2}\right) = \frac{\sigma_0}{2E_2}\left[x + \frac{L_0^*}{2\sinh(L_1/2L_0^*)}\cosh\frac{2x}{L_0^*}\right]. \quad (20)$$

This is the deformation in the constraining layer in the x direction.

We now define an equivalent homogeneous medium with the same average deformation as the composite nonhomogeneous material. For thin layers, σ_y is negligible; the effective moduli for σ_x and τ_{xy} are

$$\sigma_E^* = E_E^* \epsilon_E^*$$

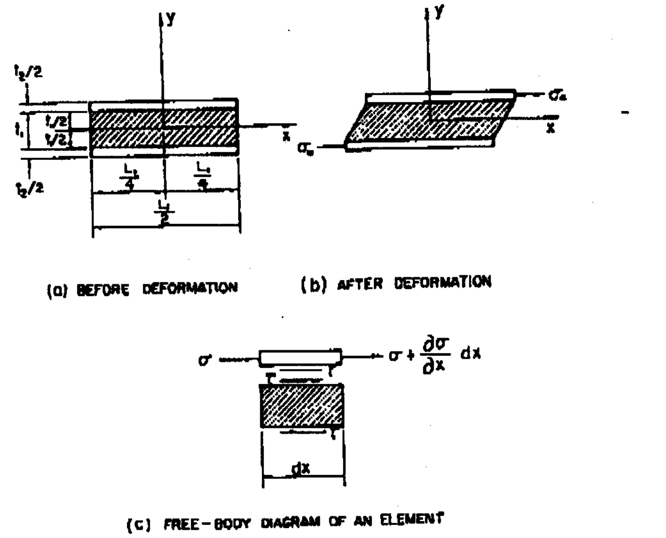

(a) BEFORE DEFORMATION (b) AFTER DEFORMATION

(c) FREE-BODY DIAGRAM OF AN ELEMENT

FIG. 6. Equilibrium of a typical volume.

and

$$\tau_E^* = G_E^* \gamma_E^*.$$

The average normal stress over the cross section is

$$\sigma_E^* = \sigma_0 t_2/2(t_1+t_2)$$

[Fig. 6(b)], and the effective normal strain is the total displacement over the quarter length divided by $L_1/4$. Using Eq. 20, we find

$$\epsilon_E^* = \frac{u^*(L_1/4, t_1/2)}{L_1/4} = \frac{\sigma_0}{2E_2}\left(1 + \frac{1}{\alpha^*}\coth\alpha^*\right),$$

where $\alpha^* = L_1/2L_0^*$; therefore,

$$E_E^* = E_2 \cdot \left(\frac{t_2}{t_1+t_2}\right)\left[1 + \frac{1}{\alpha^*}\coth\alpha^*\right]^{-1} \quad (21)$$

is the effective Young's modulus of the equivalent homogeneous material.

The actual shear stress is that in the viscoelastic layer:

$$\tau_E^* = G_1^* \cdot \frac{u^*(x, t_1/2)}{t_1},$$

and the average shear strain is

$$\gamma_E^* = \frac{u^*(x, t_1/2)}{t_1 + t_2},$$

then

$$G_E^* = G_1^* \frac{t_1 + t_2}{t_1}. \quad (22)$$

This is the effective shear modulus of the equivalent homogeneous material. Equations 21 and 22 give the

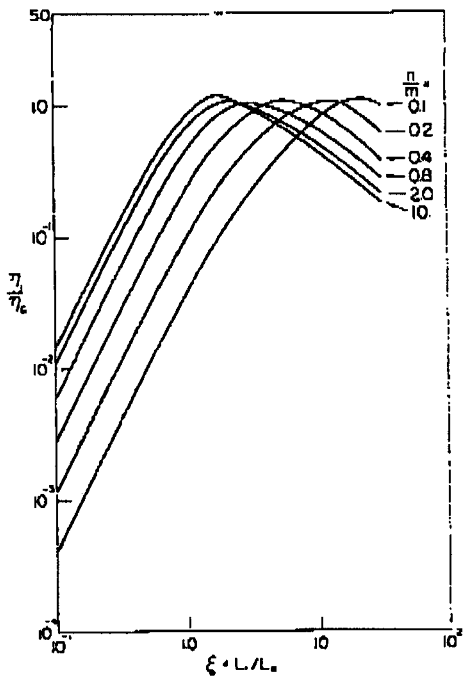

FIG. 7. η_1/η_G vs $\xi = L_1/L_s$; Layer ratio n/m as a parameter. $\eta_G \leq 0.1$.

effective moduli of the equivalent homogeneous medium in terms of the dimensions and material properties of the constituent layers of the nonhomogeneous material.

The equation of equilibrium for an element of the equivalent homogeneous orthotropic medium in terms of displacement is:

$$\partial^2 u^*/\partial x + C^{*2}(\partial^2 u^*/\partial y) = 0, \tag{23}$$

where $C^{*2} = G_E^*/E_E^*$.

Using the coordinate system as shown in Fig. 5 we obtain the boundary conditions:

(i) The strain at the interface is uniform,

$$u^*(x,0) = \epsilon_0 x;$$

(ii) The shear stress on the top surface is zero,

$$(\partial u^*/\partial y)(x,H) = 0;$$

(iii) Normal stresses at the ends vanish,

$$\frac{\partial u^*}{\partial x}\left(\pm\frac{L}{2}, y\right) = 0.$$

The general solution to Eq. 23 satisfying the boundary conditions is

$$u^*(x,y) = \epsilon_0\left\{x - \sum_{k \text{ odd}} \frac{8H\cdot\sinh[(k\pi C^*/2H)x]}{C^* k^2\pi^2 \cosh[k\pi C^* L/4H]} \times \sin\left(\frac{k\pi}{2H}y\right)\right\}. \tag{24}$$

The strain energy in the surface treatment is the work done on it through the interface between the basic structure and the treatment. Since the only force acting on the treatment is the shear stress at the interface, the strain energy is the work done by this shear force:

$$W^* = 2\int_0^{L/2} \tau_E^*(x,0)u^*(x,0)\cdot dx; \tag{25}$$

since the surface treatment is symmetric about $x=0$.

Substituting the stress–strain relation

$$\tau_E^* = G_E^*\gamma_E^*,$$

where

$$\gamma_E^* = \frac{\partial u^*}{\partial y} = \sum_{k \text{ odd}} \frac{4\epsilon_0\cdot\sinh[(k\pi C^*/2H)x]}{C^* k\pi \cosh[(k\pi C^* L/4H)]}\cdot\cos\left(\frac{k\pi}{2H}y\right)$$

and $u^*(x,0) = \epsilon_0 x$, for uniform strain at the interface, into Eq. 25 and integrating along the length, we have

$$W^* = 8\epsilon_0^2 H\cdot L\cdot E_E^* \sum_{k \text{ odd}} \frac{1}{k^2\pi^2}\left[1 - \frac{1}{k\beta^*}\tanh(k\beta^*)\right], \tag{26}$$

where

$$\beta = \frac{L}{H}\cdot\frac{\pi}{4}\cdot C^* = \frac{n}{m}\cdot\frac{L_1}{t_1+t_2}\cdot\frac{\pi}{4}\cdot C^*$$

and $n = L/L_1$ is the number of individual elements of the constraining layer; $m = H/(t_1+t_2)$ is the number of layers of the surface treatment.

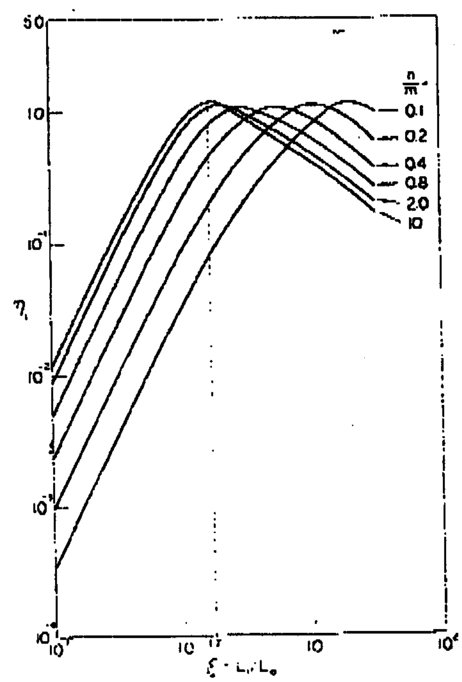

FIG. 8. η_1 vs $\xi = L_1/L_s$; Layer ratio n/m as a parameter. $\eta_G = 1.5$.

·work
basic
ıcting
·rface,
force:

(25)

=0.

ːrface,
; have

(26)

of the
ber of

$\eta_G = 1.5$.

The energy dissipation per cycle is then

$$\Delta W = \pi \cdot \mathrm{Im}(W)^*$$

$$= 8\pi\epsilon_0^2 H \cdot L \cdot E_2\left(\frac{t_2}{t_1+t_2}\right) \cdot \mathrm{Im}\left\{\left(1+\frac{1}{\alpha^*}\coth\alpha^*\right)^{-1}\right.$$

$$\left. \times \sum_{k\,\mathrm{odd}} \frac{1}{k^2\pi^2}\left[1-\frac{1}{k\beta^*}\tanh(k\beta^*)\right]\right\}. \quad (27)$$

This result is the same as would be found by evaluating

$$\Delta W = \int_V \pi G_E'' \gamma_E^2 \cdot dv,$$

as was used for single-layer analysis.

Equation 27 can be made dimensionless by dividing by a nominal energy appropriate to the system

$$W_{\mathrm{nom}} = \tfrac{1}{2}\epsilon_0^2 E_2 \cdot H \cdot L \cdot (t_2/t_1+t_2). \quad (28)$$

This would be the total strain energy in the constraining layers of the surface treatment if the whole treatment were strained by an amount ϵ_0. The dimensionless loss coefficient is then

$$\eta_1 = \Delta W / W_{\mathrm{nom}}$$

$$= 16 \cdot \pi \cdot \mathrm{Im}\left\{\left(1+\frac{1}{\alpha^*}\coth\alpha^*\right)\right.$$

$$\left. \times \sum_{k\,\mathrm{odd}} \frac{1}{k^2\pi^2}\left[1-\frac{1}{k\beta^*}\tanh(k\beta^*)\right]\right\}. \quad (29)$$

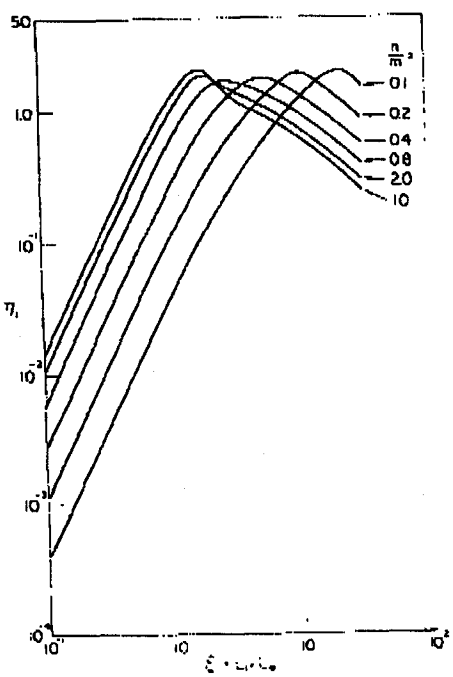

FIG. 9. η_1 vs $\xi = L_1/L_0$; Layer ratio n/m as a parameter, $\eta_G \geq 10$.

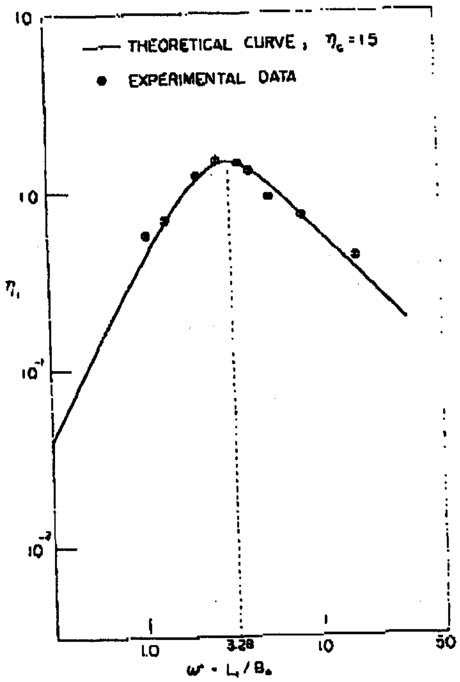

FIG. 10. Comparison of theoretical predictions and experimental results for single constraining layer.

Equation 29 indicates that the dimensionless loss coefficient η_1 is a function of α^* and β^*. But

$$\beta^* = \frac{n}{m}\cdot\frac{\pi}{2}\cdot\alpha^*\left[1+\frac{1}{\alpha^*}\coth\alpha^*\right]^{\frac{1}{2}}$$

and

$$\alpha^* = \frac{L_1}{2L_0^*} = \frac{\xi}{2}\left(\cos\frac{\theta}{2} - i\sin\frac{\theta}{2}\right),$$

where $\xi = L_1/L_0$.

Figures 7, 8, and 9 show η_1 as a function of ξ for different η_G with n/m as a parameter.

For comparison purposes, we can derive the loss coefficient for the case of a cantilever beam in flexural vibration with small deformation in the same manner as in Sec. I; the modified loss coefficient for the system is:

$$\eta_L = \eta_1 \cdot \frac{3E_2 \cdot m \cdot t_2}{\pi E_b \cdot d} \cdot \int_a^{a+L} \left(\frac{d^2y}{dx^2}\right)^2 \cdot dx \Big/ \int_0^l \left(\frac{d^2y}{dx^2}\right)^2 \cdot dx. \quad (30)$$

This is exactly the same as Eq. 14 with t_2, for single-layer treatment, replaced by mt_2 for multiple-layer treatment. The above integral is evaluated for an explicit case in Sec. III and the results are compared with measured values.

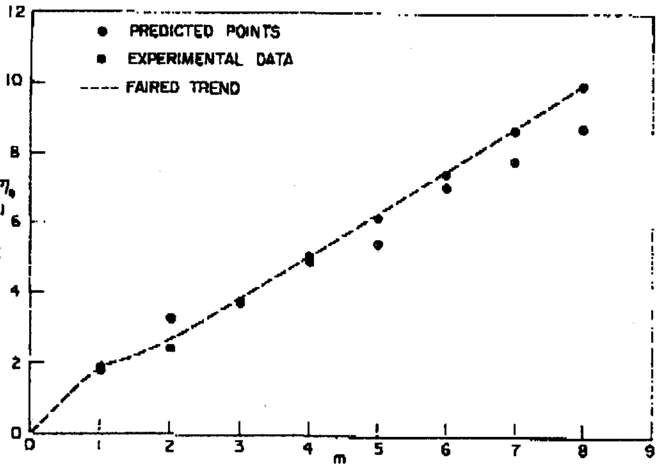

FIG. 11. Comparison of theoretical predictions and experimental results for multiple constraining layers.

III. EXPERIMENTAL RESULTS AND COMPARISON WITH THEORETICAL PREDICTIONS

Vibration decay measurements were made on a number of different cantilever beams, each with the same total length of the constrained viscoelastic-layer damping treatment but with different element lengths for comparison with the loss coefficient given by Eq. 14 for a single layer. For the multiple-layer treatment, one through eight layers were used, each with the same number of elements. The basic structure was a C1018 steel beam 7 in. long, $\frac{1}{2}$ in. wide, and $\frac{1}{8}$ in. thick; 0.0007-in.-thick aluminum foil was used as constraining layer. For the constrained viscoelastic layer, we used No. 466 3M adhesive which is 0.002 in. thick. Material properties of this adhesive were found from the master curves furnished by 3M Company. $\eta_G=1.5$ and $G_1=250$ psi (at a frequency of 66 cps and at room temperature) were used in calculations. The surface treatment was applied to the middle 4 in. of both faces of the basic structure. The test specimen was clamped at one end to a massive base isolated from the floor by foam rubber springs. The free length of the specimen was 6 in. An accelerometer attached to the free end of the cantilever beam gave an electrical signal proportional to the amplitude of free vibration. A magnetic driver was used to drive the beam at the required amplitude. After steady-state resonant vibration of the required amplitude was reached, power to the driver was cut off and the logarithmic decrement was measured.

A level recorder was used to record the envelope of the decay curve in a logarithmic scale. The slope of this curve is directly proportional to the loss coefficient

$$\eta_B \text{ or } \eta_S=\frac{\log_e 10}{20\pi f}\cdot\frac{d(\text{dB})}{dt},$$

where $[d(\text{dB})/dt]$ is the slope of the decay curve in decibels per second. Since the dissipation in the constrained viscoelastic layer cannot be measured directly, we must find it from the energy dissipation in the bare specimen without surface treatment, ΔW_B, and the energy dissipation in the test specimen with surface treatment, ΔW_S. The energy dissipation in the constrained viscoelastic layer alone is the difference between these two, $\Delta W_L=\Delta W_S-\Delta W_B$. For very thin layer surface treatment, we assume that the maximum strain energy in the system is the same for both the bare specimen and the test specimen with surface treatment, i.e., $W_S=W_B$. Then the loss coefficients for these two cases are:

$$\eta_S=\Delta W_S/2\pi W_S$$

and

$$\eta_B=\Delta W_B/2\pi W_B=\Delta W_B/2\Pi W_S.$$

We have the modified loss coefficient of the viscoelastic material in this system to be the difference between the loss coefficient of the bare specimen, η_B, and the loss coefficient of the test specimen with surface treatment, η_S:

$$\eta_L=\eta_S-\eta_B.$$

Using the measured values of η_B and η_S, and Eq. 14 and the dimensions and material properties of the test specimen used, the equivalent loss coefficient for uniform strain is

$$\bar{\eta}_1=0.803\times10^{-3}(\eta_S-\eta_B). \qquad (31)$$

The constraining layer was cut at regular intervals and measurements were made for a number of different values of L_1. The values of the dimensionless loss coefficient η_1 found from the measured $(\eta_S-\eta_B)$ are plotted in Fig. 10. For the configuration used, $t_1=0.002$ in., $t_2=0.0007$ in., $G_1=250$ psi, and $E_2=10\times10^6$ psi; therefore $B_0=0.236$ in. A theoretical curve for η_1, as found from Eq. 10 using $\eta_G=1.5$, is shown in the same figure.

For multiple-layer treatment more than one constrained viscoelastic layer is applied to each of the surfaces of the basic structure. Each subsequent constraining layer overlaps the previous one; in this particular

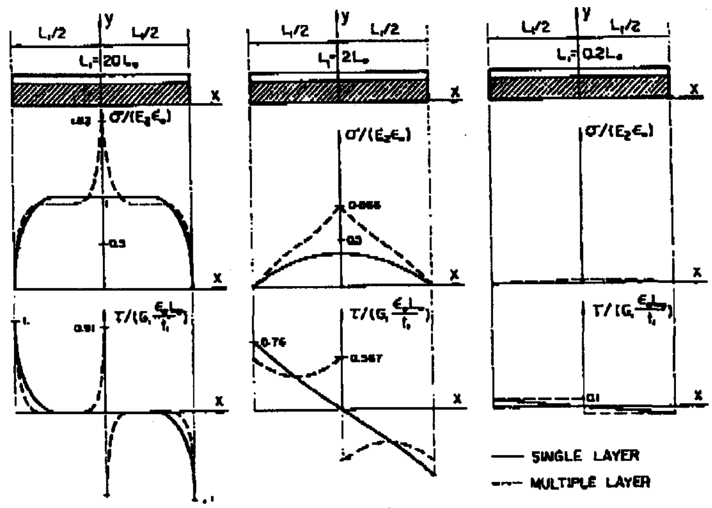

FIG. 12. Stress distribution in the surface treatment.

test, a length of $L_1=\frac{2}{3}$ in. was used for each element of the constraining layer except at the ends. In this case, $a=\frac{1}{6}$ in. and $L=4\frac{1}{2}$ in.

The measured loss coefficient $(\eta_S-\eta_B)$, is plotted against the number of layers, m, in Fig. 11. From Eq. 30, using the dimensions and properties of the test specimen gives

$$(\eta_S-\eta_B)=1.24\times10^{-3}\cdot m\cdot\eta_1, \qquad (32)$$

where η_1 is found from Fig. 8. L_0 is still 0.236 in., and L_1 is 0.667 in.; therefore, $\xi=2.82$. In this case, n, the number of elements, is 6.5 and m is the number of constraining layers. For $m=1$, η_1 is given by single layer-analysis (Fig. 10); $(\eta_S-\eta_B)$ is plotted in Fig. 11 for $m=1$ to 8 for values calculated from Eq. 32. Since the values of η_1 for $m\geq2$ are not found by the same method as that for $m=1$, the points do not fall on a smooth curve.

IV. DISCUSSION

In the analysis presented above, it has been assumed that the viscoelastic layer has a much smaller elastic modulus than the constraining layer and that the constraining layer is nondissipative. The geometric effects which change the over-all damping primarily influence the distribution of strain and extension in the constraining layer, and these interactions may be best understood by examining the appropriate functions in some detail.

For the single-layer treatment, the axial stress in the constraining layer is

$$\sigma^*=E_2(\partial u^*/\partial x),$$

where u^* is the displacement in the x direction. Using Eq. 6, we have

$$\sigma^*=E_2\epsilon_0\left[1-\frac{\cosh(x/B_0^*)}{\cosh(L_1/2B_0^*)}\right]. \qquad (33)$$

The shear stress in the viscoelastic layer is found from Eqs. 3 and 6:

$$\tau^*=G_1^*\cdot\frac{\epsilon_0B_0^*}{l_1}\cdot\frac{\sinh(x/B_0^*)}{\cosh(L_1/2B_0^*)}. \qquad (34)$$

Figure 12 shows $\sigma^*/(E_2\epsilon_0)$ and $\tau^*/[G_1^*\cdot(\epsilon_0B_0^*/l_1)]$ as functions of x with L_1 as a parameter. For large L_1, the central portion of the constraining layer undergoes the same axial strain, ϵ_0, as in the basic structure; there is no shear in the viscoelastic layer away from the ends and the damping is small [Fig. 12(a)]. For very small L_1, the elements of the constraining layer exert no constraint on the underlying viscoelastic layer, there is little shear strain, and the damping is again small [Fig. 12(c)]. At some intermediate value of L_1, the integral of the shear-strain energy integrated over the length reaches a maximum value per unit length [Fig. 12(b)] and the relative energy dissipation is maximum.

The normal stress in the constraining layer and the shear stress in the viscoelastic layer for multiple-layer treatment are found from Eq. 20:

$$\sigma^*=E_2\cdot\frac{\sigma_0}{2E_2}\left[1+\frac{\sinh(2x/L_0^*)}{\sinh(L_1/2L_0^*)}\right] \qquad (35)$$

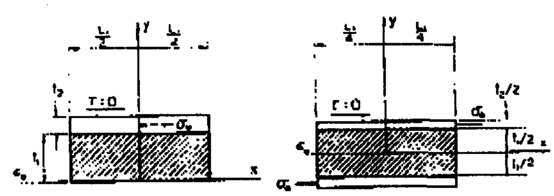

FIG. 13. Geometry of comparable boundary-value problems.

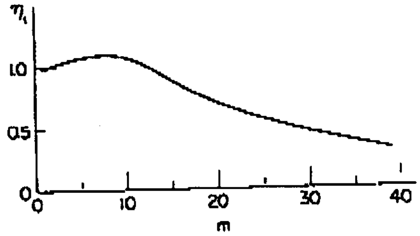

FIG. 14. η_1 as a function of m.

and

$$\tau^*=G_1^*\cdot\frac{\sigma_0}{2E_2}\cdot\frac{L_0}{t_1}\cdot\frac{\cosh(2x/L_0^*)}{\sinh(L_1/2L_0^*)}. \qquad (36)$$

To compare these results with those for single layers, we need the ratio between σ_0 and ϵ_0 (Eq. 21):

$$\epsilon_0=\frac{\sigma_0}{2E_2}\left(1+\frac{1}{\alpha^*}\coth\alpha^*\right)$$

Equations 35 and 36 can then be written as

$$\frac{\sigma^*}{E_2\epsilon_0}=\left(1+\frac{1}{\alpha^*}\coth\alpha^*\right)^{-1}\left[1+\frac{\sinh(2x/L_0^*)}{\sinh\alpha^*}\right] \qquad (37)$$

and

$$\frac{\tau^*}{G_1^*\cdot(\epsilon_0 L_0^*/t_1)}=\left(1+\frac{1}{\alpha^*}\coth\alpha^*\right)^{-1}\cdot\frac{\cosh(2x/L_0^*)}{\sinh(L_1/2L_0^*)}. \qquad (38)$$

The existence of an optimum value of L_1 for maximum damping follows from the same argument as for the single-layer treatment. Equations 37 and 38 are plotted in Fig. 12 for comparison with single-layer treatment.

For a given constraining and viscoelastic layer, there is an optimum length for the elements of the constraining layer. While the optimum length increases indefinitely as the number of layers increases, there is a minimum value as the number of layers decreases. This minimum optimum length is about half of the optimum length for a single layer of exactly the same geometry and material because the assumptions of the multiple-layer theory make the viscoelastic layer effectively stiffer. The geometry and boundary conditions of the two comparable composite configurations are shown in Fig. 13. For both problems, we have assumed that the strain is uniform at $y=0$, which is the interface of the basic structure and the viscoelastic layer in the single-layer case and is the middle surface of the viscoelastic layer in the multiple-layer case. In the single-layer analysis, $\tau=0$ at $y=(t_1+t_2)$, and $\sigma=\sigma_0$ at $x=0$, $y=t_1$. In the multiple-layer analysis, $\tau=0$ at $y=\frac{1}{2}(t_1+t_2)$ and $\sigma=\sigma_0$ at $x=L_1/4$, $y=t_1/2$; the only other difference is that $u=0$ at $x=0$, $y=0$ for the single layer but $u\neq 0$ at $x=L_1/4$, $y=0$ for the multiple-layer analysis. To make a legitimate comparison, it is necessary to replace t_1 by $2t_1$ and t_2 by $2t_2$ in the definition of L_0^* to obtain the value of B_0^* for the case of the single-layer treatment; That is,

$$L_0=2\left(t_1\cdot t_2\frac{E_2}{G_1}\right)^{\frac{1}{2}}=2B_0$$

or

$$w=L_1/B_0=2L_1/L_0=2\xi.$$

This is verified in part by the fact that the optimum element length for the single-layer case is $3.28B_0$, while for large n/m values in the multiple-layer case it is about $1.7L_0$, which is about the same physical length if the previous convention is used.

The value of w for maximum damping in the case of single-layer treatment is almost independent of the viscoelastic material used. In the case of multiple-layer treatment, the value of ξ for maximum damping changes with the number of layers and so does the length of each element of the constraining layer. It can be seen from Fig. 8 that a given value of the dimensionless loss coefficient, η_1, for a given constraining and viscoelastic layer can be obtained either with a small L_1 and few layers, m, or a large L_1 and many layers. The maximum value of η_1 for optimum ξ does not depend markedly on the number of layers which is given by the ratio m/n. Thus, from Eq. 30, the modified loss coefficient of the system, η_L, is almost linearly proportional to the number of layers if the element length is increased as the number of layers is increased. In actual applications, it is not practical to use different element lengths for different numbers of layers. If a fixed element length is used for multiple-layer treatment, the amount of damping always increases with the number of layers but not necessarily proportionally. The predicted values of $(\eta_S-\eta_B)$ for $L_1=0.667$ in. and $L_0=0.236$ in. are shown in Fig. 11, where $(\eta_S-\eta_B)$ is almost exactly proportional to m for $m=1$ to 15. This linear relation will not hold for large m because η_1 decreases for large m for this particular geometry as shown in Fig. 14.

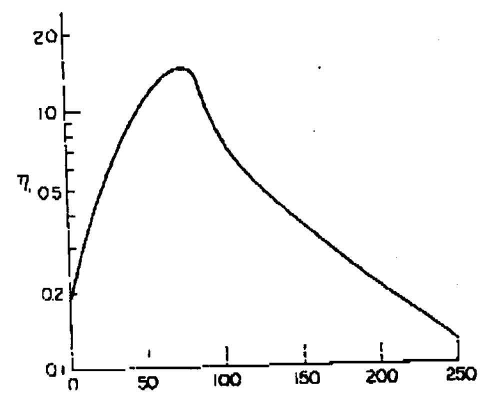

FIG. 15. η_1 as a function of temperature.

The multiple-layer theory is valid if the element length of the constraining layer is much shorter than the total length of the surface treatment. If L_1 approaches L, the strain at the middle surface of the viscoelastic layer will not be uniform, assumptions used in the derivation of the equivalent homogeneous material will be violated, and the damping will be overestimated.

In Eqs. 14 and 30, the shear modulus of the viscoelastic material does not appear explicitly; the loss coefficient of the system depends primarily upon the stiffness of the constraining layer and the strain energy of the basic structure and only indirectly on the shear modulus of the viscoelastic layer through the element length ration L_1/L_0. Viscoelastic materials with high loss factors like 3M No. 466 usually have a shear modulus which is very temperature dependent. If the element length, L_1, is chosen to be optimum for the center of the temperature range, the system damping can be designed to be almost constant over a large temperature range in spite of this. For example, if L_1 is chosen so as to make L_1/L_0-optimum at 65°F, η_1 is still as great as one-half of its maximum value at 30°F and 110°F, even though the shear modulus changes by a factor of 30 to 1 over this same range. Figure 15 shows η_1 as a function of temperature for 3M No. 466 adhesive with values of G_1 and η_G furnished by 3M Company.

V. CONCLUSION

The experimental results given in this paper agree with the damping predicted for constrained viscoelastic layers based upon the assumption that the energy dissipation is caused primarily by the shear strain in the viscoelastic layer. The effective elastic modulus method used in the analysis of a multiple-layer treatment proved to be satisfactory for the study of laminated structures. One important result found from the analysis is that, for optimum element length of the constraining layer, the energy dissipation depends primarily upon the loss coefficient of the viscoelastic material and the stiffness of the constraining layer, and only indirectly on the shear modulus of the viscoelastic layer.

ACKNOWLEDGMENT

This work was supported by the Air Force Materials Laboratory, Wright–Patterson Air Field. Permission to publish is gratefully acknowledged.

[1] E. M. Kerwin, Jr., "Damping of Flexural Waves by a Constrained Viscoelastic Layer," J. Acoust. Soc. Amer. 31, 952–962 (1959).

[2] G. G. Parfitt, "The Effect of Cuts in Damping Tapes," Int. Cong. Acoust., 4th, Copenhagen, pp. 21–28 (Aug. 1962).

[3] G. J. Lazan, A. F. Metherell, and G. Sokol, "Multiple-Band Surface Treatments for High Damping," AFML-TR-65-269 (Sept. 1965).

[4] H. Oberst, "Über Die Dampfung Der Biegeschwingungen Dunner Bleche Durch Fest Haftende Belage," Acustica 2, 181–194 (1952).

[5] E. M. Kerwin, Jr., "Macromechanism of Damping in Composite Structures," ASTM (1965).

[6] D. Ross, E. E. Ungar, and E. M. Kerwin, Jr., "Damping of Plate Flexural Vibrations by Means of Viscoelastic Laminae," ASME, Structural Damping, 49–87 (1959).

[7] B. J. Lazan, *Damping of Materials and Members in Structural Mechanics* (Pergamon Press, New York, 1968), Chap. II, pp. 16–37.

[8] R. E. D. Bishop and D. C. Johnson, *The Mechanics of Vibration* (Cambridge U. P., Cambridge, England, 1960), Chap. 7, p. 382.

panel may be expressed in terms of the loss factor of the damping layer, the ratio of the Young's modulus of the damping layer to that of the panel under treatment, and the ratio of the thickness of the damping layer to that of the panel under treatment.[18] The graphical representation of the result is shown in Fig. 37.6, using the notation of a more general theory that treats the homogeneous single layer as a particular case. The relative damping factor of the treatment is plotted against the ratio between the treatment thickness and panel thickness. The validity of this result is limited to treatment thicknesses that are relatively small compared to the panel thickness and to damping materials for which the product of the loss factor and the stiffness of the damping layer is less than one-tenth the stiffness of the undamped panel. This means that the portions of the graph to the right of $h_2 = 1.0$ are of academic interest only and should not be used for design purposes. The result is derived for one-dimensional flexure of a uniform strip or straight-crested flexural waves in plates.

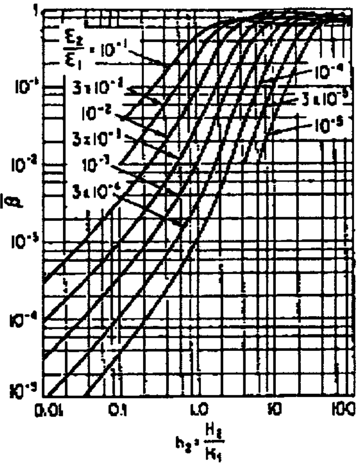

FIG. 37.6. Homogeneous adhesive viscoelastic layer theory: The relative damping factor η/β is the ratio between the loss factor of the treated panel η and the loss factor of the damping material β. The relative damping factor is plotted against the treatment thickness ratio h_2, the ratio between the treatment thickness H_2 and the panel thickness H_1. The parameter is the relative stiffness ratio between Young's modulus of the damping material E_2 and that of the panel material E_1. The subscript 1 refers to the panel, and the subscript 2 refers to the damping layer. (*After H. Oberst.*[18])

Observations from Theory. The following observations from the theory summarize its practical content. First, the loss factor of the panel treated with a mastic layer depends only on the thickness ratio between the treatment layer and the panel, rather than on the panel thickness itself. This establishes a scaling rule for comparisons of mastic layers with other classes of treatment in the laboratory. Thus the mastic thickness required on the test panel for valid ranking with other classes of material is established, once the treatment-weight limitation and panel thickness of the anticipated application have been specified. The form of the equation and slope of the curves in Fig. 37.6 show that the loss factor of the treated panel depends approximately on the square of the thickness ratio in the range of practical treatment thicknesses. Hence, the effect of the thickness of the laboratory test fixtures on the ranking of tested materials can be computed for comparison with other mechanisms of damping which may suffer less panel-thickness dependence.

Theory indicates that the optimum materials for damping must have both a high loss factor and high stiffness, because the damping factor of the treated panel depends on the loss modulus of the damping layer. The square-law dependence on thickness ratio favors application of all treatment on one side of the panel under treatment rather than dividing the weight of material between two layers on opposite sides.

Damping has been measured[14] as a function of temperature for roughly equal weights of a commercial free-layer damping material on the four structure types shown in Fig. 37.3. The thickness of the damping material was about 0.040 in. on structures A, B1, B2, and C and about 0.055 in. on D. It was attached in each case by means of a commercially available double-backed tape designed for this type of use. It will be seen (Fig. 37.7) that peak damping, whatever its specific value may be, always occurs near the same temperature, which lies near the center of the transition region for the damping material. Similar results will occur for other structures and damping materials. The

exact temperature at which peak damping occurs depend on the geometry of the structure in a manner which can sometimes be calculated; but in its broad aspects, the main controlling factor is the transition temperature of the damping material itself. This fact is most important if one is designing a damping treatment for use under conditions where the temperature can vary significantly, as in aerospace applications and in the outdoor

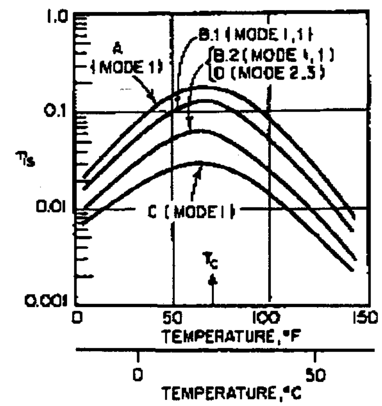

FIG. 37.7. Graphs of modal loss factor η_s vs. temperature for several structures with free layer damping. (*After D. I. G. Jones.*[14])

environment just about anywhere on earth. Internal environments in buildings may be less variable with modern heating and air-conditioning conditions, but even here some variability should be assumed.

CONSTRAINED DAMPING LAYERS

VIBRATION-DAMPING TAPES

The analysis of constrained damping layers in the form of homogeneous-adhesive tapes proceeds from certain dimensional restrictions and assumptions which are consistent with the construction of damping tapes as well as a broad class of larger-scale treatments. Among these restrictions are the following:[20] the composite bar (or plate with straight-crested flexural waves) must be thin compared with the bending wavelength so that only the damping layer is subject to shear distortion; the vibration amplitude must be small and the loss factor of the treated panel must be small; the loss modulus of the damping material must be small; the bending stiffness of the constraining layer must be small compared with that of the panel; and the Young's modulus of the damping layer must be restricted to a range between being small compared with that of the facing layers and being sufficiently large to make thickness changes in the damping layer negligible. The results of the analysis express the relative loss factor of the treated panel (the ratio between the loss factor of the treated panel η, and the loss factor η_0 of the complex shear modulus of the damping material) as a function of Young's moduli, thicknesses of the materials, and a dimensionless shear parameter g. The parameter g is the ratio between the bending wavelength and the shear length in the damping material. The shear length is the distance along the damping layer over which a local shear disturbance is reduced by a factor of $1/e$.

Engineering computations of the performance of damping tapes from shear-damping properties and dimensions of the adhesive are facilitated by families of reference curves computed for selected relative foil thicknesses. The extent of agreement between

SHOCK + VIBRATION HANDBOOK

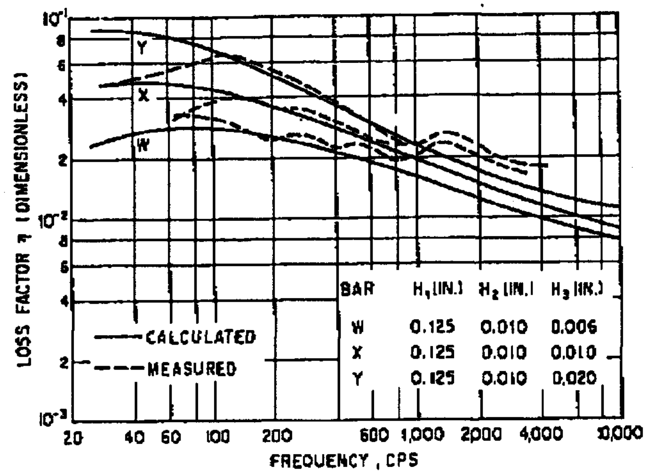

FIG. 37.8. Comparison of the measured and theoretical performance of constrained viscoelastic layers, showing the loss factor of the damped test bar at room temperature as a function of frequency for three different constraining layer thicknesses. H_1, H_2, and H_3 are the thicknesses of the bar, damping layer, and constraining layer, respectively. These results show the frequency dependence of the damping effectiveness of damping tapes. (*After E. M. Kerwin.*[10])

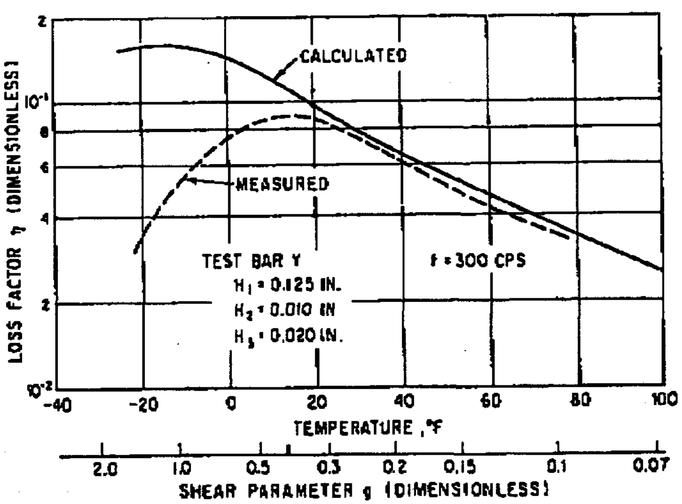

FIG. 37.9. Comparison of the measured and theoretical performance of constrained viscoelastic layers, showing the loss factor of a damped test bar at 300 cps as a function of temperature or shear parameter g (see text). H_1, H_2, and H_3 are the thicknesses of the bar, damping layer, and constraining layer, respectively. These results show the temperature dependence of the damping effectiveness of a damping tape. (*After E. M. Kerwin.*[10])

measured and calculated performance is shown in Fig. 37.8 for the case of three damping tapes applied to the same ⅛-in. bar with the same adhesive thickness of 0.010 in. but with different foil-facing thicknesses: 0.020, 0.010, and 0.006 in., respectively. The

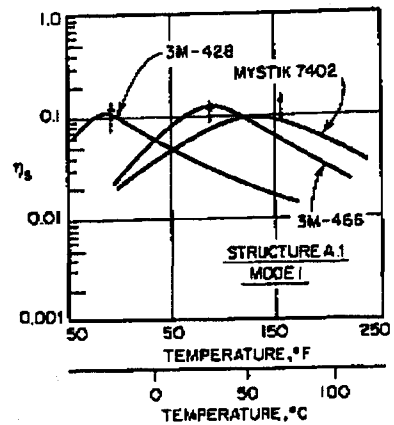

FIG. 37.10. Graphs of modal loss factor η_s vs. temperature for several multiple constrained-layer treatments. (*After D. I. G. Jones.*[11])

agreement is good over a wide range of frequency. The measured and calculated performance of one of the same tapes (0.020-in. foil backing) as a function of temperature at 300 cps is shown in Fig. 37.9. The poor agreement at low temperatures is explainable in terms of neglecting certain higher-order terms in order to facilitate computation.[10] The ability of the theory to predict shifts in the damping performance as a function of

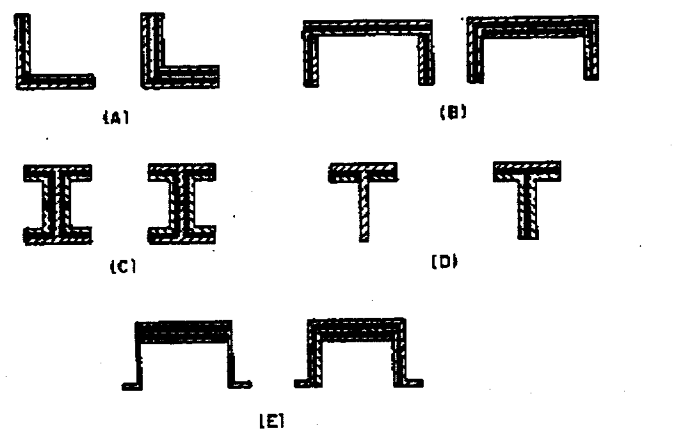

FIG. 37.11A. Cross sections of viscoelastic shear-damped composite structural beams of multilaminate construction: (*A*) angle, (*B*) channel, (*C*) I section, (*D*) T section, and (*E*) hat-section designs. (*After Ruzicka.*[26])

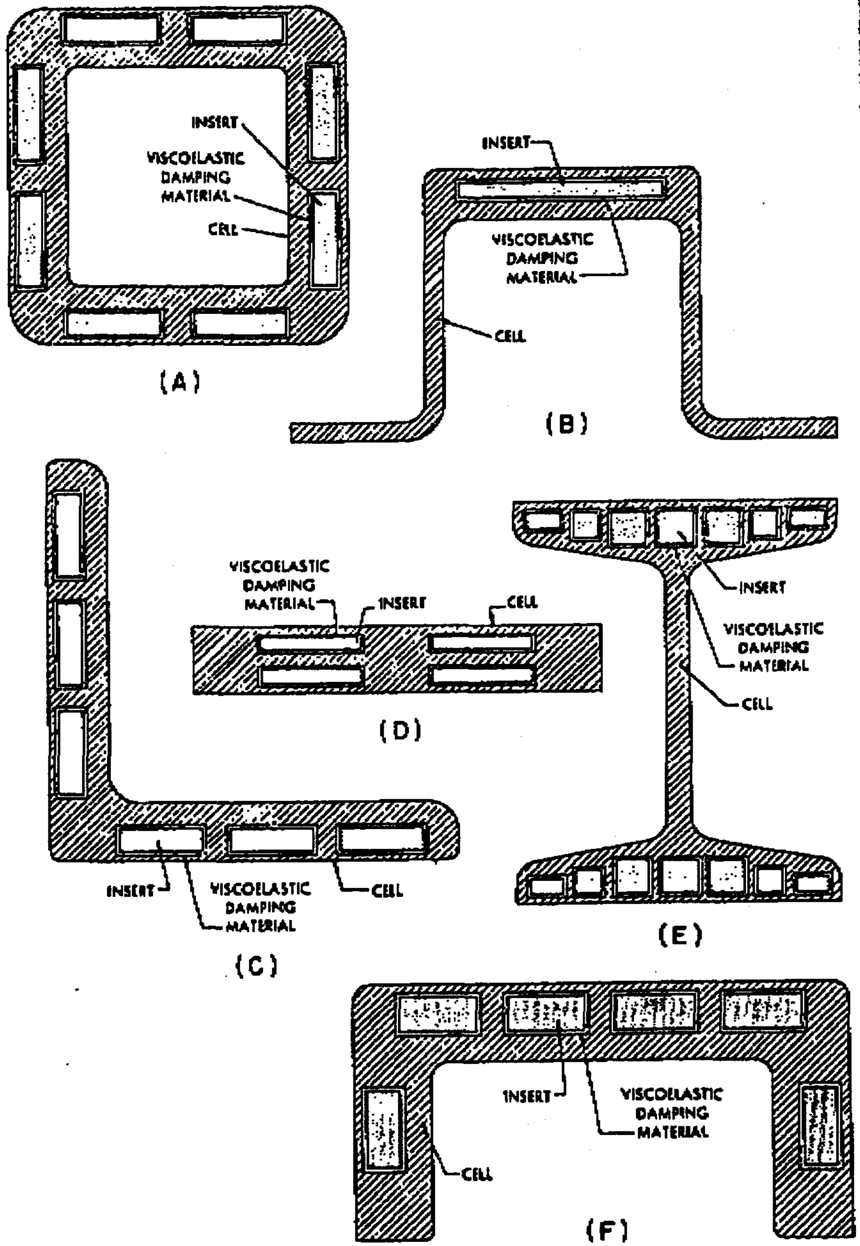

FIG. 37.11B. Cross sections of viscoelastic shear-damped composite structural beams of cell-insert construction: (A) square-tube, (B) hat-section, (C) angle, (D) flat-bar, (E) I-section, and (F) channel designs. (After Ruzicka.[23])

frequency when the same constrained layer is applied to bars of different thicknesses is also good. The scaling law involves two separate shifts of the damping-vs.-frequency characteristic: one in magnitude of damping, and the other in location along the frequency axis.

It is clearly possible to get system loss factors approaching 0.1 by optimal use of constrained elastomers. The importance of using the elastomer with the correct critical temperature is shown in Fig. 37.10. This shows the damping in a clamped-clamped beam with various five-layered treatments fully covering the surface and with adhesive thickness of 50 micron (μ) and aluminum constraining layer thickness of about 50μ. The peak loss modulus is not as significant as the transition temperature, since changes in loss modulus may be compensated for by changing the elastomer thickness.

GENERAL REFERENCES

As has been mentioned earlier, new damping materials are constantly being developed. Since their properties depend strongly on frequency and temperature, it is important to obtain the manufacturer's specifications. Manufacturers' names and addresses can be found in various annual buyers guides, including those issued by *Sweet's*, *Aviation Week*, and *Sound and Vibration* magazines. The journals of the Acoustical Society of America, The American Society of Mechanical Engineers, the Society of Environmental Engineers, the Institute of Noise Control Engineering and the other journals cited in the list of references are also fruitful sources of current information.

The *Shock and Vibration Digest*, a publication of SVIC, Naval Research Laboratory, Washington, D.C., is a unique source of reviews of the current literature as well as review articles in the field. Two review articles covering the technical literature were published in 1966; one covered the properties of materials, members, and composites[12] and the other covered the methods of measurement and analysis of system damping.[13]

References 24 and 25 are extensive compilations of the damping to be expected for structural composites with viscoelastic shear-damping mechanisms. The results are presented in dimensionless graphical form with supporting derivations and equations. Graphs are given for a wide range of viscoelastic loss factors and are easily interpreted for size and frequency. A representative but by no means exhaustive set of cross sections is shown in Fig. 37.11.

REFERENCES

1. Crandall, S. H.: *J. Sound Vibration*, 11:3-18 (1970).
2. Jacobsen, L. S.: *Trans ASME*, APM-52-15 (1930).
3. Snowden, J. C.: "Vibration and Shock in Damped Mechanical Systems," John Wiley & Sons, Inc., New York, 1968.
4. Plunkett, R.: *J. Appl. Mech.*, 30(9):70-75 (1963).
5. Plunkett, R.: *Shock and Vibration Bull.*, 42(4, NRL):67-64 (1972).
6. Lazan, B. J.: "Damping of Materials and Members in Structural Mechanics," Pergamon Press, New York, 1968.
7. Den Hartog, J. P.: "Mechanical Vibrations," chap. 8, McGraw-Hill Book Company, New York, 1956.
8. Goodman, T. P.: *J. Eng. Ind.*, 85:17 (1963).
9. Adams, R. D.: *J. Sound Vibration*, 23:199-216 (1972).
10. Birchon, D.: *Eng.*, 222:207-209 (1966).
11. Weismann, G. F., and W. Babington: *J. Environ. Sci.*, 9(5):19-27 (1966).
→ 12. Lee, L. T.: A Graphical Compilation of Damping Properties of Materials, AFML-TR-66-169, AFSC, Wright-Patterson, 1966.
13. Zener, C.: *Phys. Rev.*, 52:230-235 (1937).
14. Jones, D. I. G.: *Sound and Vibration*, 6(7):25 (1972).
15. Ferry, J. D.: "Viscoelastic Properties of Polymers," John Wiley & Sons, Inc., New York, 1970.
16. Sridharan, P., and R. Plunkett: *Trans ASME*, 96(B 3):969-975 (1974).
17. Beranek, L. L. (ed.): "Noise and Vibration Control," chap. 11, McGraw-Hill Book Company, New York, 1971.

18. Ungar, E. E.: *J. Sound Vibration*, 26:141–154 (1973).
19. Oberst, H.: *Acustica*, 2, *Akust. Beih.*, 4:181 (1952).
20. Kerwin, E. M.: *J. Acoust. Soc. Am.*, 31:952 (1959).
21. Plunkett, R., and C. T. Lee: *J. Acoust. Soc. Am.*, 46(1):150–161 (1970).
22. Lazan, B. J.: Damping Properties of Materials, Members and Composites, in "Applied Mechanics Surveys," Spartan Books, Washington, D.C., 1966.
23. Plunkett, R.: Vibration Damping, in "Applied Mechanics Surveys," Spartan Books, Washington, D.C., 1966.
24. Derby, T. F., and J. E. Ruzicka: *NASA Rept.* CR-1269, 1969.
25. Ruzicka, J. E., et al.: *NASA Rept.* CR-742, 1967.

38

TORSIONAL VIBRATION IN RECIPROCATING MACHINES

Frank M. Lewis
Massachusetts Institute of Technology

INTRODUCTION

The crankshaft of a reciprocating engine and all the moving parts driven by it comprise a torsional elastic system. Such a system has several modes of free torsional oscillation. Each mode is characterized by a natural frequency and a pattern of relative amplitudes of parts of the system. The harmonic components of the driving torque excite vibration of the system in its fundamental modes. If the frequency of any harmonic component of the torque from a single cylinder is equal to or near the frequency of any fundamental mode of vibration, a condition of resonance exists and the engine is said to be running at a *critical speed*. Operation at such critical speeds can be very dangerous, resulting in fracture of the shafting; operation at other critical speeds may result in rapid wear of bearings, gear, and other parts, and may result in undesirable vibration of the engine and associated machinery.

The number of complete oscillations of the elastic system per unit revolution of the crankshaft is called the *order of a critical speed*. The orders of critical speeds that correspond to the harmonic components of the torque from the engine as a whole are called *major orders*. Critical speeds also can be excited which correspond to the harmonic components of the torque curve of a single cylinder. Since the fundamental period of the torque from a single cylinder in a four-cycle engine is 720°, the criticals in a four-cycle engine can be of ½, 1, 1½, 2, 2½, etc., order. In a two-cycle engine, only the criticals of 1, 2, 3, etc., order can exist. All criticals except those of the major orders are called *minor criticals*, a term which does not imply that they are necessarily unimportant.

Example 38.1. A six-cylinder four-cycle engine with 120° crank spacings has three equally spaced firing impulses per revolution. The major orders therefore are 3, 6, 9, 12, etc.

The critical speeds occur at

$$\frac{f_n}{q} \quad \text{rps} \tag{38.1}$$

where f_n is the natural frequency of one of the modes in cps and q is the order number of the critical. While many critical speeds exist in the operating range of an engine, only a few are likely to be of any importance.

A dynamic analysis of an engine consists of:

1. Calculation of the natural frequencies of the modes likely to be of importance. Generally, the calculation may be limited to the lowest mode or the lowest two modes, but in some complicated arrangements more modes may be needed.
2. Estimates of the vibration amplitude at the critical speeds which are in or near the operating range.
3. A study of remedial measures if any are needed.

v) READY TO PLACE ORDER FOR VITON IN STANDARD ISOLATOR MOUNTS BARRY CONTROLS, YORK, LORD, VANGUARD

b) <u>ENCAPSULATED COMPOSITE</u>

i) $f_0 \leq 3$ Hz ISOTROPIC, LOWER X_{RMS} REDUCTION IN DRIFT

ii) HELICAL COMPOSITE SPRING IN TENSION

POSSIBLE SOURCE → a) E GLASS FIBER IN EPOXY ELASTOMER MATRIX ENCAPSULATED IN SS TUBE

A+M COMPOSITES, MALBOND MASS

b) NYLON/KEVLAR "ROPE" IMPREGNATED WITH VISCOELASTIC POLYMER, METAL PLATED

B.F. GOODRICH, TAYCO CORP

3) <u>MECHANICAL SYSTEM</u>

USE ALUMINUM OPTICAL TABLES IN 5 METER PROTOTYPE AS ISOLATED MASS 66 Kg

USE 4 S.S. ANNULAR RINGS 1" THICK AS INTERMEDIATE STAGES

FINITE ELEMENT MODEL

HONEYCOMB SANDWICH

MCI - HEXCELL
JIM WALTERS 818-961-9971

BRAZING OR WELDING

BRAZING FURNACE 48" x 100"

COSTS ≈ $400/sq ft